Eur. Phys. J. B **40**, 129–136 (2004)
DOI: 10.1140/epjb/e2004-00251-5

THE EUROPEAN PHYSICAL JOURNAL B

# Electrical resistivity in the ferromagnetic metallic state of La-Ca-$MnO_3$: Role of electron-phonon interaction

D. Varshney[a] and N. Kaurav

School of Physics, Vigyan Bhawan, Devi Ahilya University, Khandwa Road Campus, Indore 452017, India

Received 5 February 2004 / Received in final form 8 April 2004
Published online 12 August 2004 – 

**Abstract.** The temperature-dependent resistivity of the perovskite manganites $La_{1-x}Ca_xMnO_3$, with $x = 0.33$, is theoretically analysed within the framework of the classical electron-phonon model of resistivity, i.e., the Bloch-Gruneisen model. Due to inherent acoustic (low-frequency) phonons ($\omega_{ac}$) as well as high-frequency optical phonons ($\omega_{op}$), the contributions to the resistivity have first been estimated. The acoustic phonons of the oxygen-breathing mode yield a relatively larger contribution to the resistivity compared to the contribution of optical phonons. Furthermore, the nature of phonons changes around $T = 167$ K exhibiting a crossover from an acoustic to optical phonon regime with elevated temperature. The contribution to resistivity estimated by considering both phonons, i.e. $\omega_{ac}$ and $\omega_{op}$, when subtracted from thin film data, infers a power temperature dependence over most of the temperature range. The quadratic temperature dependence of $\rho_{diff.} = [\rho_{\exp.} - \{\rho_0 + \rho_{e\text{-}ph}(= \rho_{ac} + \rho_{op})\}]$ is understood in terms of electron-electron scattering. Moreover, in the higher temperature limit, the difference can be varies linearly with $T^{4.5}$ in accordance with the electron-magnon scattering in the double exchange process. Within the proposed scheme, the present numerical analysis of temperature dependent resistivity shows similar results as those revealed by experiment.

**PACS.** 5.47.Gk Colossal magnetoresistance – 72.15.-v Electronic conduction in metals and alloys – 74.25.Kc Phonons – 75.30.Ds Spin waves

## 1 Introduction

Interest in the doped perovskite manganites $R_{1-x}A_xMnO_3$ ($R^{3+}$ = La, Pr, Nd; $A^{2+}$ = Ca, Sr, Ba) has been revived due to the identification of metal-insulator (MI) and ferromagnetic transitions from the phase diagram. Quite generally these systems are regarded as spin-charge-lattice coupled metal oxides and tremendous amount of work has been carried out in some detail recently to elucidate the low temperature transport [1]. However, manganites are at the centre of research activity, since the pioneering work of Jonker and Van Santen, who noticed that the resistance below the magnetic ordering, the Curie temperature ($T_c$), exhibits a positive thermal coefficient, indicating metallic-like behaviour and a negative gradient above $T_c$ [2]. Later on, the suggestion that Zener-type [2] double exchange (DE) between spin-aligned $Mn^{3+}$ ($t_{2g}^3 e_g^1$) and $Mn^{4+}$ ($t_{2g}^3$) ions through oxygen ions gives rise to metallic conductivity and ferromagnetism was also proposed [3].

The temperature dependence of the resistivity of the doped manganites has been viewed as an important clue in the understanding of the mechanism involved. Millis et al. [4] argued that a Hamiltonian containing only double exchange is insufficient to account for large magnetoresistance observed in these compounds and suggested that a strong electron-phonon interaction mediated by Jahn-Teller (JT) coupling is essential. Furthermore, the electron-phonon coupling for the hopping process is significant as revealed from the measurements of neutron cross section for coherent elastic scattering [5]. That is why investigations of the electrical transport of doped manganites could, therefore, contribute much to the understanding also of electronic structure, role of phonons and so on.

Quite generally, the Raman and neutron scattering spectroscopy are believed to be important in probing the lattice and spin excitations and their impact on transport properties. To ascertain their significance, Abrashev et al. [6] analyze the polarized Raman spectra of $La_{0.7}Ca_{0.3}MnO_3$ thin films whose lowest optical mode has an equivalent temperature of (≈330 K) (230 $cm^{-1}$), and the broad Raman peaks centered near 470, 480 and 610 $cm^{-1}$ display a correlation with the resistivity of the sample. It is argued that these bands correspond to lattice vibrations activated by the dynamic Jahn-Teller distortions and have significant contribution to the resistivity. Moreover, other previous studies [7] on parent $LaMnO_3$ showed strong broad lines in the 450 to 600 $cm^{-1}$ range

[a] e-mail: vdinesh33@rediffmail.com; dvboson.sop@dauniv.ac.in

which were assigned to vibrations activated by the dynamic Jahn-Teller distortion. Hence, Raman spectroscopic studies point to the significant role of electron-phonon interactions in the DE mechanism for the material under consideration. On the other hand, neutron scattering measurements favor the spin-wave excitations below $T_c$ for ferromagnetic phase transition [8].

The electrical resistivity as a function of temperature in doped manganites exhibits three regimes: low-temperature metallic like conduction with an unexpectedly large absolute value of the resistivity, an abrupt drop in resistivity associated with magnetic ordering, and high-temperature activated conduction. Electron-electron, electron-magnon scattering and polaronic effects are the major proponents of various regimes in electrical resistivity behavior of doped manganites. It was first pointed out by Kubo and Ohata [9] that the perfect spin polarization of conduction electrons makes a qualitative change in the scattering processes of charge carriers by magnon-electron interactions, leading to $T^{4.5}$ dependence in a DE system. It is worth referring to an earlier work of Urushibara et al. [10], who have reported the resistivity data of $La_{1-x}Sr_xMnO_3$, and fitted their data with the quadratic temperature dependent contribution for resistivity, an indicative of electron-electron interaction. In continuation, Schiffer et al. [11] showed that in $La_{1-x}Ca_xMnO_3$ for a wide range of doping concentrations, that the resistivity for $T < 0.5\ T_c$ is well fitted by the empirical expression $\rho(T) \propto T^{2.5}$ and ascribed to usual electron-electron scattering.

However, Jaime et al. [12] ruled out the possibility of electron-electron scattering as the conduction mechanism and proposed single magnon scattering, which causes the power temperature dependent resistivity of conventional ferromagnets. The resistivity is essentially temperature independent below 20 K and exhibits a strong $T^2$ dependence above 50 K in accord with the fact that the coefficient of the $T^2$ term is about 60 times larger than that expected for electron-electron scattering. The model calculations with single magnon scattering can explain the reported data qualitatively but no quantitative agreement is established. The above results suggest that the electron-magnon scattering may be expected to be an important cause of resistivity in the metallic state.

An alternative explanation of the low-temperature electrical transport [13] of doped manganites is the polaronic effects due to electron-phonon coupling arose from dynamic JT effect, based on an argument that polarons remain predominant charge carriers even below $T_c$, and that transport is dominated by polaron tunneling. The analysis of Zhao and coworkers [13] following the small polaronic transport with soft phonons ($\approx$60 cm$^{-1}$) consistently retraces the resistivity data of $La_{1-x}Ca_xMnO_3$ below 100 K. The theory, based on a polaron picture, thus demonstrates the lowest optical modes to be significant for electrical resistivity, in contrast to the recent Raman spectroscopy measurements [6]. We also quote the work of Oleś and Feiner who stressed the importance of electron correlation, believed to be one of the important key factors controlling the transport properties in doped manganites [14].

Previously, the role of high-energy optical phonons as evident from Raman scattering measurement has been incorporated when fitting the temperature dependent resistivity in ferromagnetic state of $La_{0.67}Ca_{0.33}MnO_3$. It is the purpose of the present investigation to explore the possibility of high-energy optical phonons associated with the bending and stretching modes of octahedra in order to estimate the temperature dependent resistivity, in contrast to the previous theoretical work using the soft optical phonon mode [13] incorporating the magnitude and temperature dependence of resistivity. Also, we aim to identify the contribution of electron and spin excitations apart from lattice excitations in the transport mechanism of doped manganites.

The present investigations are organized as follows. In Section 2, we introduce the model and sketch the formalism applied. Later on, we supply technical details to estimate the phonon contribution to resistivity and support them by simple physical arguments before summarizing our results. The Debye and Einstein temperatures are obtained following the inverse-power overlap repulsion for nearest-neighbour interactions in an ionic solid. We employ the Bloch-Gruneisen method to estimate the independent contributions of acoustic and optical phonons. In Section 3, we return to the details of numerical analysis and discussion of results obtained by way of resistivity curves.

The major findings include: (i) acoustic phonons of the oxygen breathing mode yield a relatively large contribution to the resistivity compared to the contribution of optical phonons; (ii) the quadratic temperature dependence of $\rho_{diff}[= \rho_{\exp} - (\rho_0 - \rho_{e\text{-}ph})]$ is interpreted in terms of electron-electron scattering in the low temperature domain (85 K $\leq T \leq$ 160 K), following a $T^{4.5}$ dependence at elevated temperature in accord with the scattering of electron-electron and electron-magnon. Here the notation $\rho_0$ symbolizes the residual resistivity. The successful fitting of $\rho(T)$ for the test material clearly demonstrates the validity of the approach and infers that it may be useful in analyzing the lattice contribution to $\rho\ (T)$ in other doped manganites.

The final part of the paper is devoted to conclusions and is presented in Section 4. The effects of electron-electron and electron-magnon scattering are substantial enough to yield a right shape of the temperature-dependent resistivity and in fairly good agreement with experiments. It is worth noticing that the detailed information on physical parameters in correlated electron system, such as manganites can be understood by electrical transport phenomenon.

## 2 Method of calculations

We start by briefly describing the electronic structure of perovskite $La_{1-x}Ca_xMnO_3$. The bandwidth of the conduction band is primarily determined by the overlapping of the manganese and oxygen. The larger the overlap, the

wider the band. For a given distance between the manganese and oxygen ions the overlap is largest when the Mn-O-Mn bond angle is 180°. This occurs when a manganese and six oxygen ions form regular octahedra. But if lanthanum is replaced with a smaller ion, the octahedra buckle and the bond angle becomes smaller. The structural instability in La-Ca-MnO arises out of the twofold orbital degeneracy of $Mn^{3+}$ leading to optical breathing-mode vibration of oxygen atoms. In this respect, elastic coupling of these vibrations at individual sites stabilizes cooperative distortions which can be either long or short range. We anticipate that both acoustic and optical phonons participate in the process of electrical conduction.

We begin by discussing the phonon mechanism.

### 2.1 Estimation of Debye and Einstein temperature

The interpretation of the experimental data is in the framework of the electron-phonon interaction using the model phonon spectrum consisting of acoustic branch of Debye type and a widely separated optical peak with characteristic Einstein temperature. Usually, the ideal cubic structures perovskite $ABO_3$ posses around fifteen normal modes of vibration. The Raman measurements yield the phonon spectrum that consists of a triply degenerate acoustical mode at the zone center, and three infrared (IR) active optical modes allowed for cubic symmetry. These phonon modes are classified as external, bending or stretching modes depending on the energy scale. The lowest frequency (external mode) corresponds to a vibration of the $A$ ions against the rigid $BO_6$ octahedra. The intermediate frequency (bending mode), corresponds to a vibration where the $B$ ion and two apical oxygens move against the other four oxygens of the octahedron. At the highest frequency (stretching mode), the $B$ ion moves against the rigid oxygen octahedron [15].

With these facts in mind, we choose a model phonon spectrum along the conducting Mn-O plane consisting of two parts: an acoustic Debye branch characterized by the Debye temperature $\theta_D$ and an optical peak defined by the Einstein temperature $\theta_E$. The Debye frequency is characterised as a cut off frequency at the Brillouin zone boundary, and it can be expressed in terms of effective value of ionic mass and elastic force constant for crystal lattices with two different kind of atoms such as Mn and O, which we deal with. The acoustic-mode and optical-mode frequencies are estimated in an ionic model using a value of effective ion charge $Ze = -2e$. The Coulomb interactions among the adjacent ions in an ionic crystal in terms of inverse-power overlap repulsion as [16]

$$\Phi(r) = -(Ze)^2 \left[\frac{1}{r} - \frac{f}{r^s}\right], \tag{1}$$

$f$ being the repulsion force parameter between the ion cores. The elastic force constant $\kappa$ is conveniently derived from $\Phi(r)$ at the equilibrium inter-ionic distance $r_0$ following

$$\kappa = \left(\frac{\partial^2 \Phi}{\partial r^2}\right)_{r_0} = (Ze)^2 \left[\frac{s-1}{r_0^3}\right]. \tag{2}$$

Here, $s$ is the index number of the overlap repulsive potential. We choose an acoustic mass $M' = (2M_+ + M_-)$ [Mn (O) is symbolised by $M_+(M_-)$], $\kappa^* = 2\kappa$ for each directional oscillation mode to get the acoustic phonon frequency as

$$\omega_D = \sqrt{\frac{2\kappa^*}{M'}}, = 2(Ze)\sqrt{\frac{(s-1)}{M'}\frac{1}{r_0^3}}. \tag{3}$$

Furthermore, when the phonons belong to optic modes, their frequency is determined by the reduced mass as $\mu^{-1} = M(\mathrm{Mn})^{-1} + M(\mathrm{O})^{-1}$ [17]

$$\omega_{LO}^2 = \frac{\kappa + \eta}{\mu} \tag{4}$$

and

$$\omega_{TO}^2 = \frac{\kappa - \eta}{\mu} \tag{5}$$

where $\eta$ is the force constant as

$$\eta = \frac{8\pi}{3}\frac{(Ze)^2}{\Omega} \tag{6}$$

$\omega_{LO}$ ($\omega_{TO}$) indicates the longitudinal (transverse) optical phonon frequency and $\Omega$ the volume of the unit cell.

We proceed to include the temperature dependent resistivity for $La_{0.67}Ca_{0.33}MnO_3$ manganites.

### 2.2 Metallic resistivity

To formulate a specific model, we start with the general expression for the temperature dependent part of the resistivity, given by [18]

$$\rho = \frac{3\pi}{\hbar e^2 v_F^2} \int_0^{2k_f} |v(q)|^2 \left\langle |S(q)|^2 \right\rangle \left(\frac{1}{2k_F}\right)^4 q^3 dq \tag{7}$$

$v(q)$ is the Fourier transform of the potential associated with one lattice site, $v_F$ being the Fermi velocity and $S(q)$ is the structure factor. Following the Debye model it takes the following form

$$|S(q))|^2 \approx \frac{k_B T}{M v_s^2} f(x) \tag{8}$$

$$f(x) = x[e^x - 1]^{-1}[1 - e^{-x}]^{-1} \tag{9}$$

$f(x)$ represents the statistical factor with $x = \hbar\omega/k_B T$.

Thus the resistivity expression leads to

$$\rho \approx \left(\frac{3}{\hbar e^2 v_F^2}\right)\frac{k_B T}{M v_s^2}\int_0^{2k_F} |v(q))|^2 \left[\frac{x q^3 dq}{[e^x - 1][1 - e^{-x}]}\right]. \tag{10}$$

$v_s$ being the sound velocity. Equation (10) in terms of acoustic phonon contribution yields the Bloch-Gruneisen function of temperature dependent resistivity:

$$\rho_{ac}(T,\theta_D) = 4A_{ac}(T/\theta_D)^4 \times T\int_0^{\theta_D/T} x^5 (e^x-1)^{-1}\left(1-e^{-x}\right)^{-1} dx \quad (11)$$

where, $x = \hbar\omega/k_BT$. $A_{ac}$ is a constant of proportionality defined as

$$A_{ac} \cong \frac{3\pi^2 e^2 k_B}{k_F^2 v_s^2 L\hbar v_F^2 M}. \quad (12)$$

If the Matthiessen rule is obeyed, the resistivity may be represented as a sum $\rho(T) = \rho_0 + \rho_{e\text{-}ph}(T)$, where $\rho_0$ is the residual resistivity that does not depend on temperature as electrons also scatter off impurities, defects and disordered regions. On the other hand, in the case of the Einstein types of phonon spectrum (an optical mode) $\rho_{op}(T)$ may be described as follows

$$\rho_{op}(T,\theta_D) = A_{op}\theta_E^2 T^{-1}\left[\exp(\theta_E/T)-1\right]^{-1} \times \left[1-\exp(-\theta_E/T)\right]^{-1}. \quad (13)$$

$A_{op}$ is defined analogously to equation (12). Thus, the phonon resistivity can be conveniently modeled by combining both terms arising from acoustic and optical phonons

$$\rho_{e\text{-}ph}(T) = \rho_{ac}(T,\theta_D) + \rho_{op}(T,\theta_E) \quad (14)$$

Finally, the total resistivity is now rewritten as

$$\begin{aligned}\rho(T,\theta_D,\theta_E) &= \rho_0 + \rho_{ac}(T,\theta_D) + \rho_{op}(T,\theta_E)\\ &= \rho_0 + 4A_{ac}(T/\theta_D)^4 T\\ &\quad\times\int_0^{\theta_D/T} x^5(e^x-1)^{-1}\left(1-e^{-x}\right)^{-1}dx\\ &\quad + A_{op}\theta_E^2 T^{-1}\left[\exp(\theta_E/T)-1\right]^{-1}\\ &\quad\times\left[1-\exp(-\theta_E/T)\right]^{-1}. \quad (15)\end{aligned}$$

We use the values of various physical parameters in the next section to estimate the temperature- dependent contribution. The Coulomb correlations and spin wave excitations are also important in manganites for resistivity apart from electron-phonon scattering, which we discuss in the next section.

## 3 Discussion and analysis of results

For the actual calculation of the transport properties, it is essential to know realistic values of some physical parameters governing the resistive behaviour. Any discussion of the manganites necessitates knowledge of the crystal structure, and this is particularly true of the calculations documented here. There can be orthorhombic, rhombohedral and cubic phases in entire range of doping both as a function of temperature and as a function of concentration. While calculating the Debye temperature, we take $s = 8$ and the in plane Mn-O distance $r_0 = 1.96$ Å [19] for $La_{0.67}Ca_{0.33}MnO_3$, yielding $\kappa = 11\times10^4$ gms$^{-2}$. We note that the present model has only one free parameter, i.e, index number of the repulsive potential. It is worth noting that for correlated electron systems such as cuprates, the index number of the repulsive potential has been reported to be $s = 10$ [20].

With these parameters, the Debye frequency is estimated as 35.8 meV (416 K), and is needed for estimation of the acoustic phonon contribution in temperature dependent resistivity for the doping concentration $x = 0.33$. The deduced value of the Debye temperature is consistent with the reported value from heat capacity measurements ($\theta_D$ = 430 K for $x$ = 0.33) for $La_{1-x}Ca_xMnO_3$ manganite [21]. However, this value was extracted from data at lower temperature ($T \leq 10$ K) fitted directly to the Debye function. Usually, the Debye temperature is a function of temperature and varies from technique to technique. Values of the Debye temperature also vary from sample to sample with an average value and standard deviation of $\theta_D = \theta_D \pm 15$ K. Furthermore, the optical phonon mode is obtained as $\omega_{LO} \approx 54.6$ meV (634 K) and $\omega_{TO} \approx 39.8$ meV (462 K). The calculated values of the LO/ TO frequencies are consistent with the measured values of the optical phonons from the infrared (IR) spectra of thin film and polycrystalline of $La_{0.7}Ca_{0.3}MnO_3$ [6,22]. Henceforth, the deduced coefficients ($A_{ac}$ and $A_{op}$) are 0.8 and 1.84, respectively and are comparable with the earlier deduced in the normal state resistivity of electron doped cuprates [15].

We emphasize here that the deduced frequencies of the optical modes are consistent with those observed in Raman spectra and are associated with the dynamic Jahn-Teller distortion, arising from the local lattice distortion due to the strong electron-phonon coupling. It is worth mentioning that a direct relationship has been established between the degree of the Jahn-Teller distortions of $MnO_6$ octahedra and conductivity and magnetic properties of the structure [23]. This necessarily points to the fact that the optical phonon mode can be correlated with the degree of the Jahn-Teller distortion activated modes corresponding to bending and stretching oxygen vibrations of the $MnO_6$ octahedra.

Figure 1 illustrates the results of temperature dependence of resistivity via the electron-phonon interaction from equation (14) with our earlier choice of $\theta_D$ (=416 K) and $\theta_E$ (=462 K). The contributions of acoustic and optical phonons towards resistivity are shown separately along with the total resistivity. It is inferred from the curve that $\rho_{ac}$ increases linearly, while $\rho_{op}$ increases exponentially with the increase in temperature. The contributions are summed and the resultant resistivity is exponential at low temperatures, and nearly linear at high temperatures upto room temperature. In the following calculations, we have used $\rho_0 \approx 10^{-4}$ Ω cm.

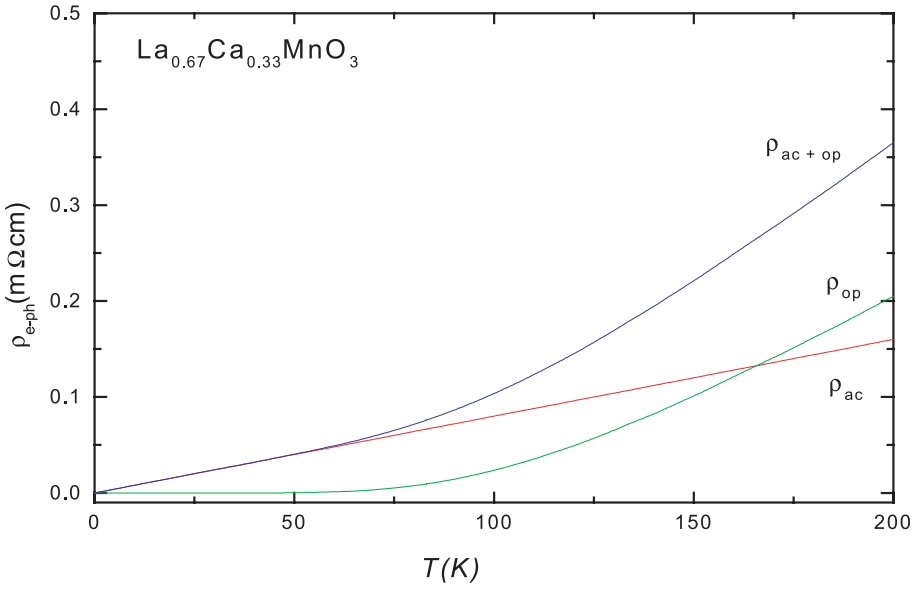


**Fig. 1.** Variation of $\rho_{e\text{-}ph}$ with temperature for $La_{0.67}Ca_{0.33}MnO_3$, the contribution of acoustic phonons $\rho_{ac}$ as well of optical phonons $\rho_{op}$ to the resistivity.

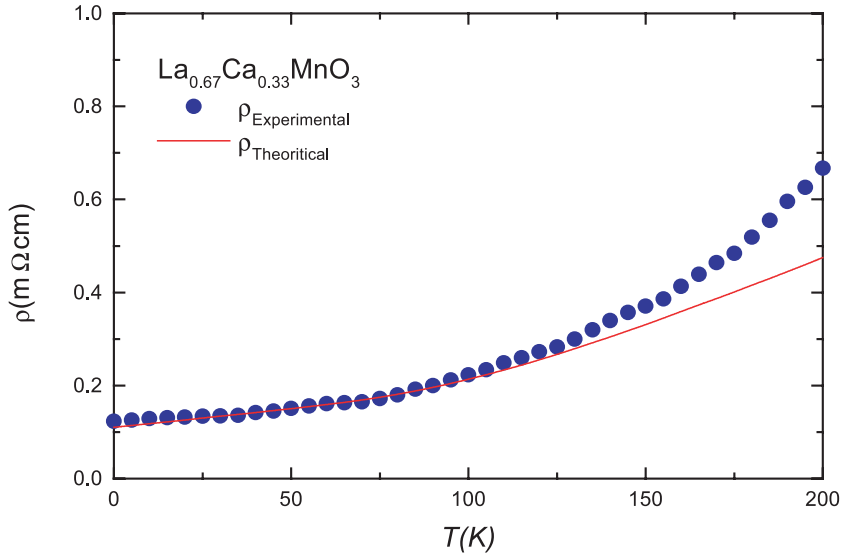


**Fig. 2.** Variation of $\rho$ with temperature $T$(K). Open circles are the experimental data taken from Snyder et al. (1996).

Our numerical results on temperature dependence of resistivity of $La_{0.67}Ca_{0.33}Mn\ O_3$, are plotted in Figure 2 along with the experimental data on thin films [24]. It is noticed from the plot that the estimated $\rho$ is lower than the reported data from $T = 100$ K to near room temperature. The model phonon spectrum with characteristic $\theta_D$ (=416 K) and $\theta_E$ (=462 K) partially reveals the reported resistivity behavior. Prior to our model calculations, Zhao and coworkers [13] have predicted that small polaronic transport is the prevalent conduction mechanism below 100 K, which involves a relaxation due to a soft optical phonon mode (86 K) that is strongly coupled to the carriers. In addition, a small contribution from acoustic-phonon would give almost perfect fit with a negligible systematic deviation. On the other hand, we use high-energy optical phonons as well acoustic phonons to retrace the reported resistivity behavior. We propose that in manganites the Raman spectrum [6] yields the lowest optical mode that has an equivalent temperature of (≈330 K), considerably higher than the polaron picture used for the fitting of resistivity data. We believe that a phonon hardening effect on the carrier transport would be expected, and would be very significant in manganites as earlier observed by Infrared Reflectivity measurement [22] in the metallic phase of $La_{0.7}Ca_{0.3}MnO_3$ and by the lattice dynamical calculations [25].

The difference between the measured $\rho$ and calculated $\rho_{diff.}[= \rho_{\exp.} - \{\rho_0 + \rho_{e\text{-}ph}(= \rho_{ac} + \rho_{op})\}]$ is plotted in Figure 3. A quadratic temperature dependence of $\rho_{diff.}$ is depicted at low temperature. The quadratic temperature contribution for resistivity is an indication of conventional electron-electron scattering. The quadratic

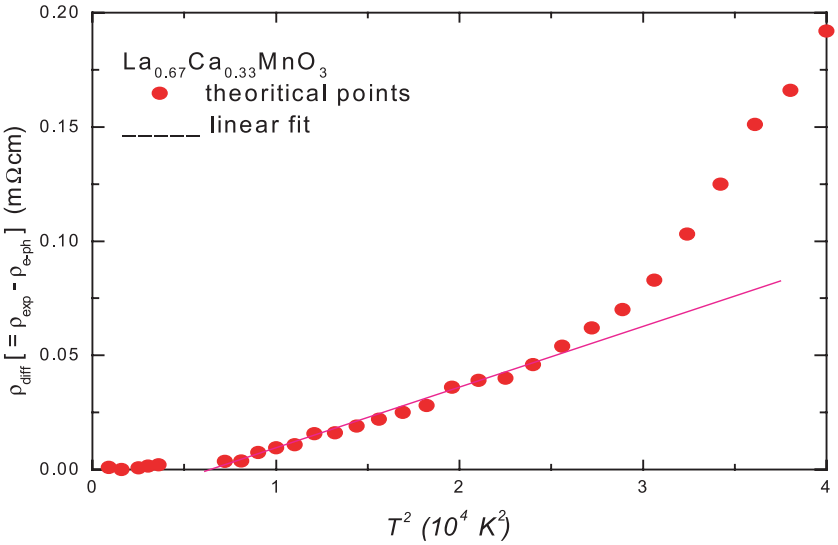


**Fig. 3.** Variation of $\rho_{diff}[= \rho_{\rm exp} - (\rho_0 + \rho_{e\text{-}ph}\{\rho_{ac} + \rho_{op}\})]$ (m Ωm) with $T^2$ ($10^4$ K$^2$).

temperature dependence of $\rho_{diff.}$ is consistent with the earlier argument made by Urushibara and coworkers [10]. The additional term due to electron-electron contribution was required in understanding the resistivity behaviour, as extensive attempts to fit the data with residual resistivity and phonon resistivity were unsuccessful. It is noteworthy to comment that in conventional metals, the electron-electron contribution to the resistivity can at best be seen only at very low temperatures, due to its small magnitude in comparison with the phonon contribution. The existence of quadratic temperature dependence of resistivity over a wide temperature interval permits one to believe that the electron-electron scattering is also significant in determining the resistivity in manganites.

In passing, we refer to an earlier work of Thompson [26], who postulated the power temperature dependence of electroresistivity in $TiS_2$ as a consequence of low carrier concentration. Furthermore, using the Fermi-liquid relation $N(\varepsilon_F) = 3n/2\varepsilon_F$, we find an upper bound of the Fermi energy of about 0.6 eV. In principle the electron-electron scattering is proportional to $(1/\varepsilon_F)^2$ and hence small Fermi energies enhance the electron-electron scattering [18]. The value of the calculations is stressed from the fact the electron-electron scattering has been predicted in a magnetic material with a low-carrier density ($\cong 10^{21}$ cm$^{-3}$) for the $La_{0.67}Ca_{033}MnO_3$ system. However, the carrier density in doped manganites is comparable to those for other perovskite oxides [27]. In addition, in low-temperature region of manganites $T \ll T_c$, where spin moments are considered to be almost saturated, the roles of orbital degeneracies have also been considered important, which may contribute to the Fermi-liquid-type $T^2$ resistivity down to zero temperature.

We now address the metallic behavior of doped manganites. If the high-frequency phonon modes, as deduced are indeed strongly coupling with charge carriers, the effective mass of the carriers should be substantially enhanced. The effective mass of the electron along the conducting Mn-O plane is deduced from electronic specific heat coefficient $\gamma$, using, $m^* = 3\hbar^2\gamma d/\pi k_B^2$. The parameters employed are $d = 7.78$ Å [19] and $\gamma = 4.7$ mJ mol$^{-1}$ K$^{-2}$ [21] to get $m^* = 2.4\ m_e$. The two dimensional charge carrier density is taken as $2.2 \times 10^{14}$ cm$^{-2}$. Henceforth, the electron parameters are estimated as the Fermi velocity $v_F$ ($=1.9 \times 10^7$ cm sec$^{-1}$) and $\omega_p$ (=2.3 eV). However, electronic energy band structure calculations [28] derive the average Fermi velocity as $7.4 \times 10^7$ cm sec$^{-1}$, much higher than our estimate from the Fermi liquid approximation. In passing, we refer to our recent work on heat capacity analysis, where it is argued that the effects induced by electron correlations and mass renormalizations by electron-electron interactions are crucial in magnetic systems such as doped manganites [29].

Quite generally, in conventional metals, electron-phonon scattering is mathematically identical to conventional impurity scattering, and leads to a resistivity proportional to $(v_F^2\ell)^{-1}$ where $\ell$ is the mean free path. The mean free path in this approximation is usually related to the Fermi velocity and is estimated following $\ell = v_F\tau$. We find $\ell$ of about 18 Å for $La_{0.67}Ca_{0.33}MnO_3$. We follow the Drude relation, $\tau^{-1} = \rho_0\,\omega_p^2/4\pi$, to obtain $\tau^{-1} = 1.05 \times 10^{14}$ s$^{-1}$. It is meaningful to mention that the residual resistance obtained for nominally the same compositions may vary significantly for different groups of compounds. Theoretically it remains unclear whether $\rho_0$ only characterizes the sample's quality or if there is an intrinsic component in the residual resistivity. The former suggestion is argued in the results of resistivity experiments [30]. However, the resistivity data for $La_{1-x}Sr_xMnO_3$ in the crystalline films yields $\rho_0$ as low as $10^{-5}$ Ωcm [10]. This is a typical metallic conductivity range. To gain an additional insight, we further deduce the product $\varepsilon_F\tau \gg 1$, that favors the doped manganites to be a good metal.

It is thus argued that the larger the electron mass ($m^* = 2.4m_e$) in correlated electron systems, the smaller the plasma frequency, and hence the reduced zero

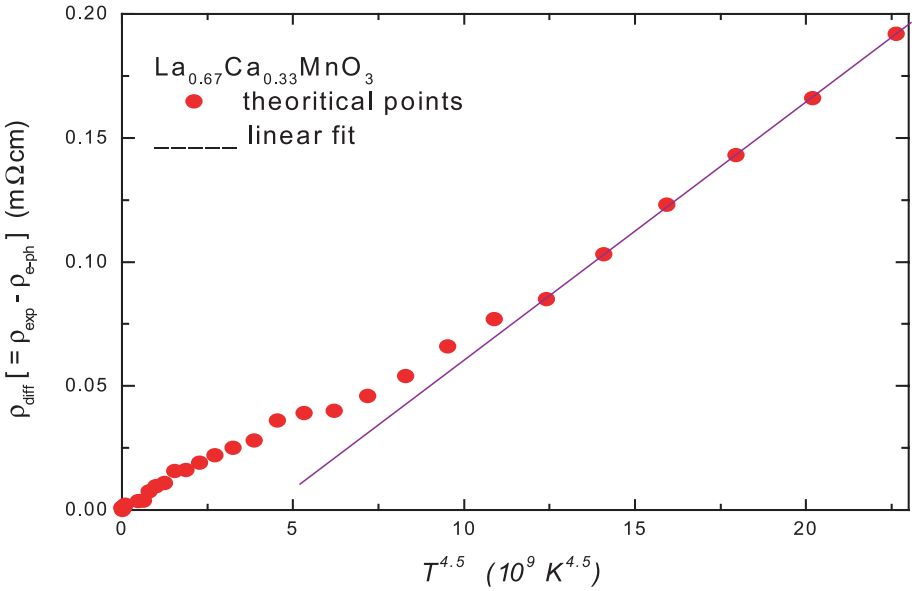


**Fig. 4.** Variation of $\rho_{diff}[= \rho_{\exp} - (\rho_0 + \rho_{e\text{-}ph}\{\rho_{ac} + \rho_{op}\})]$ (m Ω cm ) with $T^{4.5}$ ($10^9$ $K^{4.5}$).

temperature elastic scattering rate in comparison to conventional metals. It is perhaps worth noticing that, in hole-doped high-$T_c$ cuprates, the scattering rate at low temperatures is of the order of $10^{14}$ $s^{-1}$. Furthermore, the Mott-Ioffe-Regel criterion for metallic conductivity is valid, as the mean free path is several times [$\ell \cong 18$ Å] larger than the Mn-O bond length (1.963 Å [19]). A significantly enhanced mean free path is an indication of metallic conduction as the product $k_F\ell$ ($\sim$7) seems to be much larger than unity. Hence, it is appropriate to use the Bloch-Gruneisen expression in estimating the electron-phonon contributions.

Previously, Jaime and coworkers [12] emphasised electron-electron scattering as the conduction mechanism and argued for single magnon scattering leading to the power temperature dependent resistivity. Our results differ from Jaime and coworkers in that the phonon contribution which must be present is taken into account using the model phonon spectrum, and the resulting power temperature dependence of nonphonon term suggests electron-electron scattering of a more conventional type. We believe from the calculations presented here, that the $T^2$ temperature-dependent term in the low temperature domain in resistivity should not be due to single-magnon scattering. The justification lies in the fact that $La_{0.67}Ca_{0.33}MnO_3$ at low temperatures is of half-metallic character [28]. This necessarily points to the fact that the conduction is limited to a single Mn spin up channel of majority carriers. Compared to that, the Mn spin down channels are localized, and hence the normal emission and absorption of spin waves at finite temperatures are forbidden. As a result there are no conducting states at low energy to scatter into spin flip.

We again refer to Figure 3, where a substantial deviation from the $T^2$-like behavior and a rapid rise in $\rho_{diff}$ is observed in the intermediate temperature region ($T < T_c$). We perform the similar set of exercises with the difference between the measured $\rho$ and calculated $\rho_{diff.}[= \rho_{\exp.} - \{\rho_0 + \rho_{e\text{-}ph}\ (= \rho_{ac} + \rho_{op})\}]$ beyond 160 K (plotted in Fig. 4). A $T^{4.5}$ temperature dependence of $\rho_{diff.}$ is depicted at higher temperature. The $T^{4.5}$ temperature contribution for resistivity is an indication of electron-magnon scattering. In the intermediate temperature region ($160 < T < T_c$), the manganites appear to be normal metallic ferromagnet with the resistivity dominated by spin wave scattering. It is worth referring to an earlier work of Fulde and Jensen [31], who have argued that carrier density also changes by interaction with spin wave in manganites. The feature of $T^{4.5}$ temperature dependence of $\rho_{diff.}$ is consistent with the quantum theory of two-magnon scattering [9] and is valid for half-metallic ferromagnets. Consequently, besides electron-phonon and electron-electron interaction, another explanation for the variation in carrier density is the presence of spin wave in the metallic system, and is caused by spin wave scattering. We finish by stating that the proposed model calculations reproduces the reported electrical behavior with a combination of $T^2$ and $T^{4.5}$ apart from electron-phonon contribution, consistent with earlier predictions [11].

## 4 Conclusions

Either double exchange mechanisms or small polarons have primarily described the physics of manganites. The behavior of electrical resistivity in doped manganites needs more clarification. The reported behavior of electrical resistivity in doped manganites is analysed in the framework of the additional model of electron-phonon interaction using the model phonon spectrum consisting of two parts: an acoustic branch of Debye type and optical mode with characteristic Einstein temperature. Deduced values of Debye and Einstein temperatures from an overlap repulsive potential are consistent with the specific heat

and Infrared Reflectivity measurements. For the sake of simplicity, a single (longitudinal and transverse) optical phonon mode has been considered, with a flat dispersion relation.

The high-energy optical phonon yields a large contribution to the resistivity and is attributed to significant optical phonon hardening effect on carrier transport. It is noticeable that the contribution from acoustic and optical phonons together with the residual resistivity is smaller than experimental data. A clear straight line is depicted from 84 K to 160 K temperature range while plotting the difference as a function of $T^2$. The observation of power temperature dependence of resistivity points toward electron-electron scattering. The extra contribution arising from the electron-electron contribution is required in manganites to analyze the resistivity behaviour, since extensive attempts to fit the data with residual resistivity and phonon resistivity have been unsuccessful.

The mean free path is several times larger than the Mn-O bond length and the product $k_F L > 1$ favors metallic conduction. Hence, it is appropriate to use the Bloch-Gruneisen expression in estimating the electron-phonon contributions. The electron scattering rate at low temperature is inversely proportional to Fermi energy and the value of $\varepsilon_F$ is low ($\approx$0.6 eV) in doped manganites as compared to conventional metals, which implies that the low value of $\varepsilon_F$ enhances the electron-electron scattering rate at low temperatures. Deduced scattering rate at low temperatures is of the order of $10^{14}$ s$^{-1}$ in Ca-doped manganites. Hence, the identity $\varepsilon_F \tau \gg 1$ holds for manganites and again argues in favour of metallic conductivity.

In addition, we succeeded in exploring the role of electron-magnon scattering in the electrical transport mechanism. It is noticeable that the role of two-magnon scattering in the resistivity behaviour is prominent above 160 K. We propose that the incorporation of $T^{4.5}$ dependence is essential and may consistently reproduce the experimental results for the resistivity at higher temperatures. It is inferred from the above analysis that the electrical transport below $T_c$ is not dominated by electron-electron scattering, but also by electron-magnon, presumably involving spin fluctuations of charge carriers.

To conclude, the present model calculations thus lead to both qualitative and quantitative agreement between the calculated and experimental results. Although we have provided a simple explanation of these effects, there is a clear need for good theoretical understanding of the resistivity behavior, in view of the fact that formation of small polarons may be of magnetic origin in manganites.

Financial assistance from Madhya Pradesh Council of Science and Technology, Bhopal is gratefully acknowledged.

## References

1. M.B. Salamon, M. Jaime, Rev. Mod. Physics **73**, 583 (2001)
2. G.H. Jonker, J.H. Van Santen, Physica **16**, 337 (1950); J.H. Van Santen, G.H. Jonker, Physica **16**, 599 (1950)
3. C. Zener, Phys. Rev. **82**, 403 (1951); P.W. Anderson, H. Hasegawa, Phys. Rev. **100**, 675 (1955)
4. A.J. Millis, P.B. Littlewood, B.I. Shrainman, Phys. Rev. Lett. **74**, 5144 (1995); A.J. Millis, B.I. Shrainman, R. Mueller, Phys. Rev. Lett. **75**, 175 (1996)
5. P. Dai, J. Zhang, H.A. Mook, S.-H. Liou, P. A. Dowben, E. W. Plummer, Phys. Rev. B **54**, R3694 (1996)
6. M.V. Abrashev, V.G. Avanov, M.N. Iliev, R.A. Chakalov, R.I. Chakalova, C. Thomsen, Phys. Status Solidi (b) **215**, 631 (1999); M.V. Abrashev, A.P. Litvinchuk, M.N. Iliev, R.L. Meng, V.N. Popov, V.G. Ivanov, R.A. Chakalov, C. Thomsen, Phys. Rev. B **59**, 4146 (1999)
7. M.N. Iliev, M.V. Abrashev, H.G. Lee, V.N. Popov, Y.Y. Sun, C. Thomsen, R.L. Meng, C.W. Chu, Phys. Rev. B **57**, 2872 (1998)
8. J.W. Lynn, R.W. Erwin, J.A. Borchers, Q. Huang, A. Santoro, Phys. Rev. Lett. **76**, 4046 (1996)
9. K. Kubo, N. Ohata, J. Phys. Soc. Jpn **33**, 21 (1972)
10. A. Urushibara, Y. Moritomo, T. Arima, A. Asamitsu, G. Kido, Y. Tokura, Phys. Rev. B **51**, 14103 (1995)
11. P. Schiffer, A.P. Ramirez, W. Bao, S.-W. Cheong, Phys. Rev. Lett. **75**, 3336 (1995)
12. M. Jaime, P. Lin, M.B. Salamon, P.D. Han, Phys. Rev. B **58**, R5901 (1998)
13. Guo-meng Zhao, V. Smolyaninova, W. Prellier, H. Keller, Phys. Rev. Lett. **84**, 6086 (2000)
14. A.M. Oleś, Louis F. Feiner, Phys. Rev. B **65**, 052414 (2002)
15. E. Granado, N.O. Moreno, A. García, J.A. Sanjurjo, C. Rettori, I. Torriani S.B. Oseroff, J.J. Neumeier, K.J. McClellan S.-W. Cheong, Y. Tokura, Phys. Rev. B **58**, 11435 (1998)
16. D. Varshney, K.K. Choudhary, R.K. Singh, Supercond. Sci. Technol. **15**, 1119 (2002)
17. M. Born, K. Huang, *Dynamical theory of crystal lattices* (Oxford University Press – London, 1966)
18. G. Grimvall, *The Electrons-Phonon Interaction in Metals* (North-Holland Pub. Com. – New York, 1980)
19. J. Blasco, J. Garcia, J.M. de Teresa, M.R. Ibarra, J. Perez, P.A. Algarabel, C. Marquina, C. Ritter, Phys. Rev. B **55**, 8905 (1997)
20. D. Varshney, M.P. Tosi, J. Phys. Chem. Solids **61**, 683 (2000)
21. L. Ghivelder, I. Abrego Castillo, N.M. Alford, G.J. Tomka, P.C. Riedi, J. MacManus-Driscoll, A.K.M. Akther Hossain, L.F. Cohen, J. Magn. Magn. Mater. **189**, 274 (1998)
22. K.H. Kim, J.Y. Gu, H.S. Choi, G.W. Park, T.W. Noh, Phys. Rev. Lett. **77**, 1877 (1996)
23. C.H. Booth, F. Bridges, G.H. Kwei, J.M. Lawrence, A.L. Cornelius, J.J. Neumeier, Phys. Rev. Lett. **80**, 853 (1998)
24. G.J. Snyder, R. Hiskes, S. DiCarolis, M.R. Beasley, T.H. Geballe, Phys. Rev. B **53**, 14434 (1996)
25. J.D. Lee, B.I. Min, Phys. Rev. B **55**, 12454 (1997); J.D. Lee, B.I. Min, Phys. Rev. B **55**, R 14713 (1997)
26. A.H. Thompson, Phys. Rev. Lett. **35**, 1786 (1975)
27. J.M.D. Coey, M. Viret, L. Ranno, K. Ounadjela K, Phys. Rev. Lett. **75**, 3910 (1995)
28. W.E. Pickett, D.J. Singh, Phys. Rev. B **53**, 1146 (1996)
29. D. Varshney, N. Kaurav, Eur. Phys. J. B **37**, 301 (2004)
30. M. Quijada, J. Cerne, J.R. Simpson, H.D. Drew, K.H. Ahn, A.J. Millis, R. Shreekala, R. Ramesh, M. Rajeswari, T. Venkatesan, Phys. Rev. B **58**, 16093 (1998)
31. P. Fulde, J. Jensen, Phys. Rev. B **27**, 4085 (1983)